

Phase regeneration of an M-PSK signal using partial regeneration of its M/2-PSK second phase harmonic

Liam Jones*, Francesca Parmigiani, Periklis Petropoulos, David J. Richardson
Optoelectronics Research Centre, University of Southampton, Southampton, SO17 1BJ, UK
**orc.jones@soton.ac.uk*

Keywords: All-optical phase regeneration, Phase sensitive amplification, Fiber optic amplifiers and oscillators, Nonlinear optics, Parametric processes, Numerical simulations

Abstract:

We propose and numerically investigate a phase regeneration technique that allows an M-PSK signal to be phase regenerated by an M/2-PSK (or even M/4-PSK) phase regenerator (applicable for $M = 2^k$, with k an integer). This scheme comprises three main parts; firstly, phase harmonic generation is used to create the second and third phase harmonics, secondly, the second phase harmonic (a down-converted M/2-PSK signal) is partially phase-regenerated, and thirdly and finally, the partially regenerated second phase harmonic and the third phase harmonic are mixed together to re-synthesise a phase regenerated replica of the original signal.

1. Introduction

Next generation communication systems will rely on complex modulation formats in order to meet the increasing capacity demands imposed by user requirements. Complex modulation formats offer higher spectral efficiencies, however they require adherence to higher optical signal to noise ratios (OSNRs), increasing the need for signal regeneration. The electronic methods currently used for this do not scale well with increasing data rate and number of data channels. The development of all-optical techniques capable of eliminating phase noise (and ideally amplitude noise as well) from multi-level phase signals is consequently of great interest. To date, optical regeneration of binary phase shift keying (BPSK) and quadrature phase shift keying (QPSK) signals has been successfully demonstrated exploiting the characteristics of either single- or dual- pump phase-sensitive amplification (PSA), implemented in either highly nonlinear fibers (HNLF) [1-2], periodically poled Lithium Niobate (PPLN) waveguides [3-4], or semiconductor optical amplifiers (SOA) [5]. The regeneration of an M-PSK signal (where M is the number of phase levels used) is possible in principle in a dual pump PSA, but

requires the generation of higher order phase harmonics [2], posing inherent practical difficulties. Indeed, the generation of high-order phase harmonics through four-wave mixing (FWM) can be limited by the fiber parameters and input power constraints. Very recently 16-QAM signals in both polarizations and up to three channels have been successfully processed in a “copier-PSA” configuration [4], however this comes with the compromise of doubling the bandwidth occupied by the system. In the literature, a suggested approach towards the regeneration of complex modulation formats is to first demultiplex the signal into simpler phase-only tributaries, before parallel regeneration and subsequent coherent recombination [6]. In this work, we follow the same principle in order to regenerate an M-PSK signal, where $M = 2^k$, with k an integer. In our approach, we propose to generate the second and third phase harmonics in a FWM process where the M-PSK signal and a continuous wave (CW) beam are used as the pump and the FWM-seed signal, respectively. The generated second phase harmonic, which corresponds to an optically format down-converted M/2-PSK signal [7], is subsequently partially regenerated before being coherently recombined with the third phase harmonic signal in another FWM process, where the M/2-PSK signal is used as the pump, to obtain back the now fully phase-regenerated original M-PSK signal. A key point of the scheme is that regeneration of an M/2-PSK rather than an M-PSK signal is required. It is quite intuitive that this scheme can then, in principle, be repeated several times in order to scale to ever higher values of M to allow the regeneration of signals of ever increasing complexity, albeit at the expense of more involved physical implementations.

2. Principle of Operation

The operating principle of the proposed M-PSK phase regeneration scheme is depicted in Fig. 1 for the example of an 8-PSK signal. The figure also shows representations of the corresponding spectra at various points in the system. The regenerator comprises three main stages: in the first stage, the 8-PSK signal and a CW pump are used as inputs in a FWM process (a phase-insensitive amplifier, PIA) to generate the second and third phase harmonics of the incoming 8-PSK signal. If the pump phase is assumed constant for the sake of clarity, and thus ignored, the phases of the second and third phase harmonics can be written as a function of the initial 8-PSK signal as follows:

$$\phi_{second\ harmonic} = 2 * \phi_{8-PSK} \quad (1)$$

$$\phi_{third\ harmonic} = 3 * \phi_{8-PSK} \quad (2)$$

For the second phase harmonic the phase states 0 and π are changed to 0 and 2π after the process (similar relationships apply to the remaining states, as shown in Table 1) and as a consequence, the second phase harmonic corresponds to an optically format down-converted 4-PSK signal (i.e. it takes the form of a QPSK signal). This transformation is pictorially represented in Fig. 2 in the form of the signal constellation. (It should be appreciated however, that this is only a virtual format conversion, since the 4-PSK second phase harmonic signal cannot possibly contain the full information of the original 8-PSK signal.) For the third phase harmonic, on the other hand, the nominal phase values are multiplied by three, and as a result, the third phase harmonic corresponds to a signal which is still in the form of 8-PSK, but where the various symbol allocations have been shuffled in the constellation map, as also pictorially represented in Fig. 2. The corresponding nominal phase combinations between the various harmonics are also summarized in Table 1. In the second stage, the format converted QPSK signal (M/2-PSK in the general case) is partially phase regenerated. Meanwhile the third phase harmonic is simply temporally delayed to guarantee synchronization and temporal coherence with the partially regenerated second phase harmonic. Finally, in the third stage, the partially regenerated QPSK signal is coherently mixed with the third phase harmonic in order to obtain the properly regenerated 8-PSK signal. This is achieved by using them as the pump and signal, respectively, in an additional PIA stage. The phase of the mixing output $\phi_{8\text{-PSK}_{\text{output}}}$ can then be written as follows:

$$\phi_{8\text{-PSK}_{\text{output}}} = 2 * \phi_{\text{reg_second harmonic}} - \phi_{\text{third harmonic}} \quad (3)$$

If Eq.1 and Eq.2 are substituted in Eq.3, we obtain:

$$\phi_{8\text{-PSK}_{\text{output}}} = 2 * (2 * \phi_{8\text{-PSK}_{\text{input}}}) - 3 * \phi_{8\text{-PSK}_{\text{input}}} = \phi_{8\text{-PSK}_{\text{input}}} \quad (4)$$

Equation 4 implies that in the noiseless case we obtain back the original 8-PSK formatted signal.

In order to understand how regeneration is achieved, we need to write similar equations for the corresponding phase noise components associated with each of the nominal phase states. For example, if each phase state of the original signal is characterized by an initial phase error $\Delta\phi_N$ (so that the actual relative value of the phase of the symbol is $\phi_{8\text{-PSK}_{\text{input}}} + \Delta\phi_N$), the second (third) phase harmonic will have twice (three times) that phase error. Bearing this in mind and considering Eq.3, it can be deduced that to achieve optimum phase squeezing

capability (where the output phase noise is zero), i.e. the minimum phase error for each nominal phase state, it is crucial that the phase noise error of the format converted signal must only be partially regenerated (by 25%). With this partially regenerated phase error of the second phase harmonic (i.e. $2 * \Delta\phi_N$ becoming $1.5 * \Delta\phi_N$), a similar equation to Eq. 3 can be written to represent the output phase error of each state:

$$\Delta\phi_{N_OUTPUT} = 2 * (1.5 * \Delta\phi_N) - 3 * \Delta\phi_N = 0 \quad (5)$$

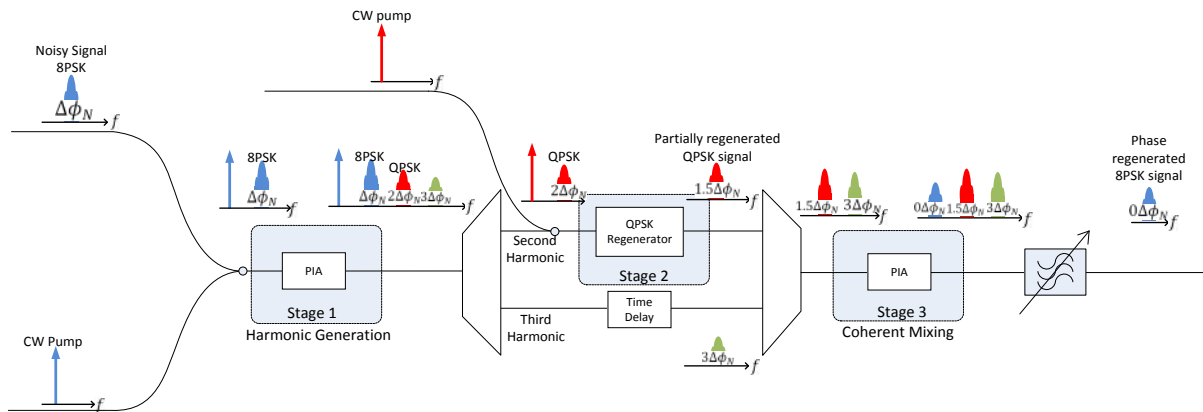


Fig. 1: Operating principle and schematic diagram of the proposed M-PSK phase regenerator, adapted for an 8-PSK signal.

This regeneration technique can be extended, such that the process of harmonic phase generation, partial regeneration and recombination can be nested to allow the use of even lower level regenerators. For instance, the QPSK signal resulting from format conversion, in the case described above, can be further converted to a BPSK signal. This BPSK signal can be partially regenerated (by a factor which can be calculated to be 6.25% following the same methodology as above) and then sequentially recombined with the third phase harmonics of each nested loop to generate the phase regenerated 8-PSK signal.

It is worth highlighting that no specific phase or frequency relation is required between the pumps in Stage 1 and Stage 2, and also that the pumps have been assumed ideal with no associated noise in the simulations.

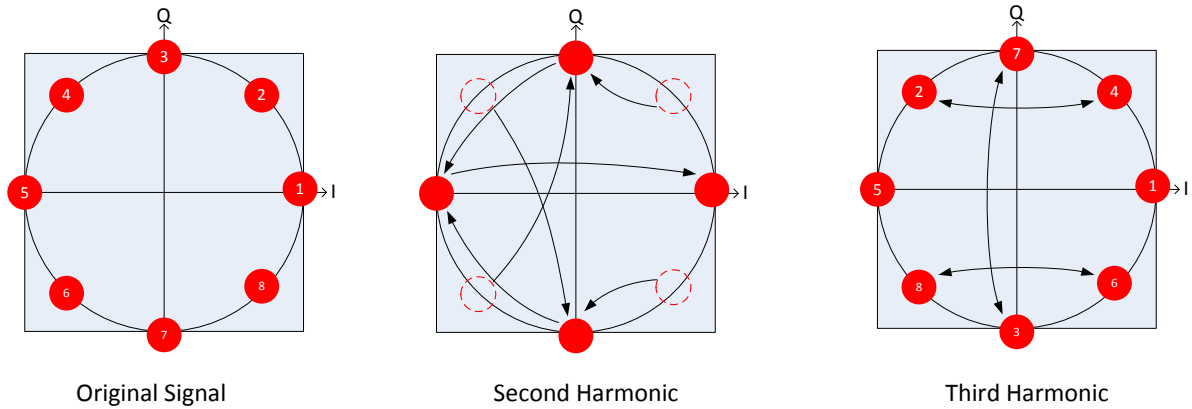


Fig. 2: Constellation diagrams showing symbol placements for original signal (left), second (middle) and third (right) phase harmonics.

Table 1: Individual symbol phase values.

Symbol	Input signal Phase	2nd Harmonic (SH) Phase	3rd Harmonic (TH) Phase	2*(SH)-(TH) Phase
1	0°	0°	0°	0°
2	45°	90°	135°	45°
3	90°	180°	270°	90°
4	135°	270°	45°	135°
5	180°	0°	180°	180°
6	225°	90°	315°	225°
7	270°	180°	90°	270°
8	315°	270°	225°	315°

3. Simulation and analysis

We carried out detailed simulations to prove the validity of our proposed approach. Our simulations assumed a set-up that followed the schematic shown in Fig.1. A non-return-to-zero (NRZ) 25 GBaud 8-PSK signal at 1557 nm was combined with a CW pump at 1552 nm before entering the phase harmonic generation stage. For the nonlinear element in the first stage, as well as in all the others included in the set-up, we used the characteristics of a state-of-the-art strained HNLFF that is readily available in our laboratories, and which exhibits a dispersion, dispersion slope, zero dispersion wavelength, nonlinear coefficient, linear loss and length of -0.08ps/nm/km, 0.018ps/nm²/km, 1553nm, 11.6/W/km, 0.88dB/km and 302m, respectively [2]. The fiber SBS threshold after straining HNLFF was 27dBm. The second and third order phase harmonics which were produced in the first PIA were then demultiplexed; the second phase harmonic, the format down-converted

QPSK signal, was partially regenerated assuming the characteristics of the dual-pump non-degenerate PSA described in [2]. The maximum power used of the two phase-locked pumps for this PSA was 24dBm each, while the power of the signal was 10dBm. These power relations ensured that the signal was only partially regenerated at the output of the PSA (optimum phase regeneration would require a power of 27dBm on each of the pumps). In parallel, the third phase harmonic was propagated through a standard single mode fiber (SSMF) in order to properly match the two paths. The partially regenerated second phase harmonic was coherently mixed with the third phase harmonic in a last PIA stage to reconstruct the 8-PSK with regenerated phase at exactly the original wavelength.

Fig. 3 reports the response of the proposed system. In particular, Fig. 3(a) shows the output phase transfer function as a function of the input signal phase between $-\pi/8$ and $+\pi/8$ radians. The blue dots represent the numerical simulations and the red line represents the analytic fit. To obtain this fit, the signals after the partial QPSK regenerator and at the very output of the system were represented by their amplitude (A_{pr} and A_{out}) and phase (ϕ_{pr} and ϕ_{out}) transfer profiles, as follows:

$$A_{pr}e^{i\phi_{pr}} \propto e^{i*(2\phi_s)} + me^{-i3*(2\phi_s)} \quad (6)$$

$$A_{out}e^{i\phi_{out}} \propto A_{pr}^2 \cdot e^{i(2\phi_{pr}-3\phi_s)} \quad (7)$$

where ϕ_s is the phase of the initial 8-PSK signal and m is the optimum mixing ratio which depends on the gain of the PSA process [2]. The optimal value for the m factor, which was used to calculate the corresponding transfer functions displayed in Fig. 3, is $m = 0.069$ ($M/2=4$). As compared to the value of $m = 0.33$ required for full QPSK regeneration (as estimated in [8]), this is lower, as expected, since only partial regeneration is needed. The system implication is that Stage 2 requires lower pump powers than an ideal QPSK regenerator, in order to achieve the optimum overall phase transfer function. However, the trend of the various transfer functions as m increases are very similar in the two regenerators, and the phase transfer functions for four values (0, 0.069, 0.13 and 0.33) of m are depicted in Fig.4. Fig. 4 a) displays the single step (between $-\pi/4$ and $\pi/4$ radians) phase transfer function for the four m values directly after the QPSK regenerator (stage 2). Fig. 4 b) displays the corresponding single step (between $-\pi/8$ and $\pi/8$ radians) phase transfer function for the four m values for the final 8PSK signal (after stage 3).

Fig. 3(b) shows the numerical simulation and analytic fit of the output amplitude as a function of the input phase between $-\pi$ and $+\pi$ radians. As expected the amplitude of the synthesized signal becomes a sinusoidal function of the phase with a periodicity of $2\pi/M$. Fig. 3(c) displays how the input signal (green) with induced continuous phase variations from 0 to 2π is shaped at the very output (blue) of the (fully regenerated) system.

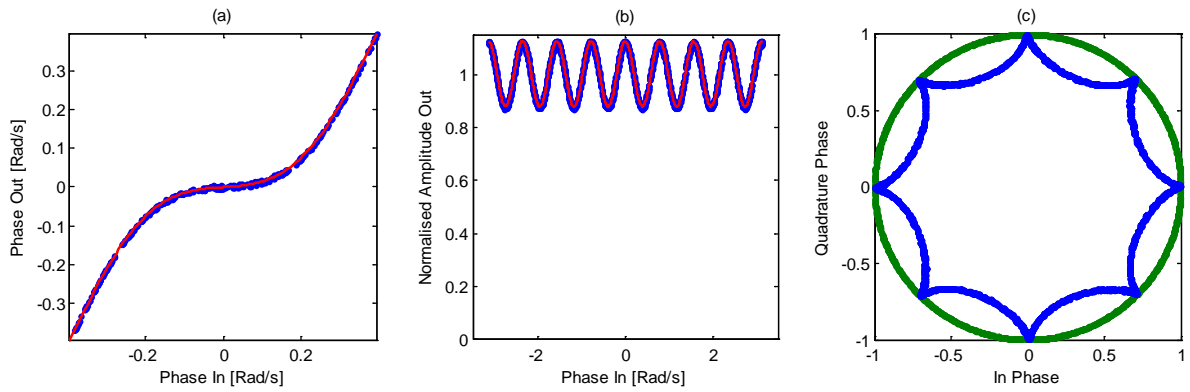


Fig. 3: Simulation in blue, analytic fit in red for a) Phase transfer function versus input phase between $-\pi/8$ and $\pi/8$ rads, b) Amplitude phase transfer function versus input phase and c) full phase spread constellation diagram of input (green) and output (blue).

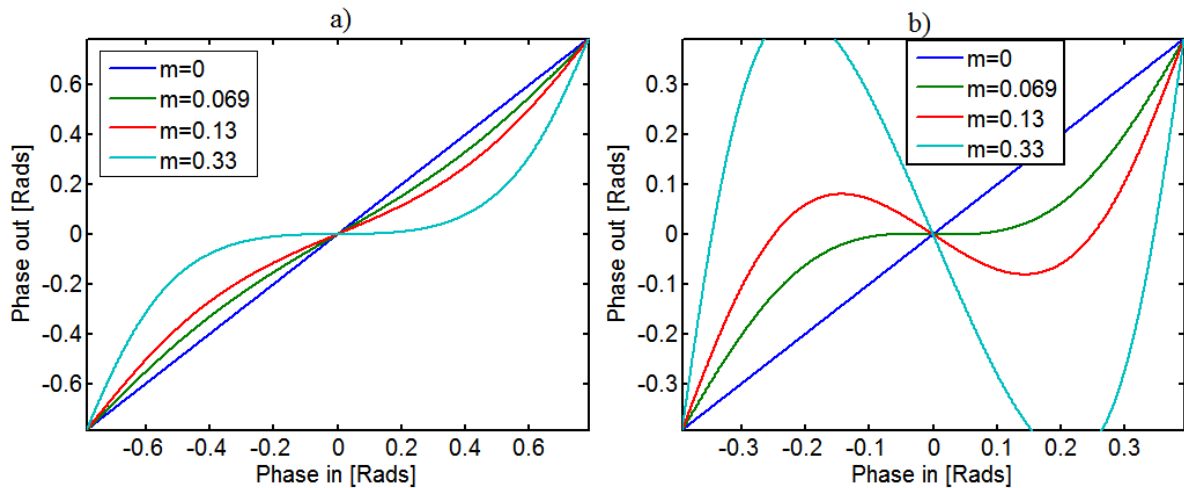


Fig. 4: Single step phase transfer function of the a) QPSK signal after stage 2, and the b) final 8PSK signal, with m factor set to 0 (blue), 0.069 (green), 0.13 (red) and 0.33 (teal)

Some better appreciation of the regenerator performance can be obtained from Figs. 5 and 6, which present corresponding constellation diagrams at the input (a) and output (b) of the 8-PSK regenerator for two different values of phase noise with a constant (flat-top) probability density function of 0.062 radians and 0.098 radians, respectively, added to the signal, neglecting any amplitude noise. At the output of the regenerator the phase noise distribution was reduced to 0.006 radians and 0.016 radians in these two respective cases.

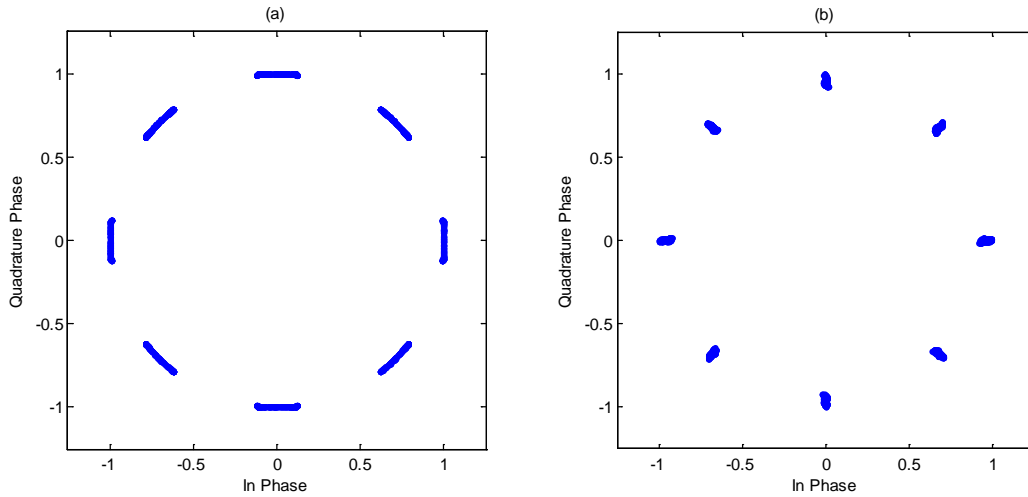


Fig. 5: Example of constellation diagrams at the input (a) and output (b) of the system when a phase noise of 0.062 radian (with a constant probability density function) is added to the signal.

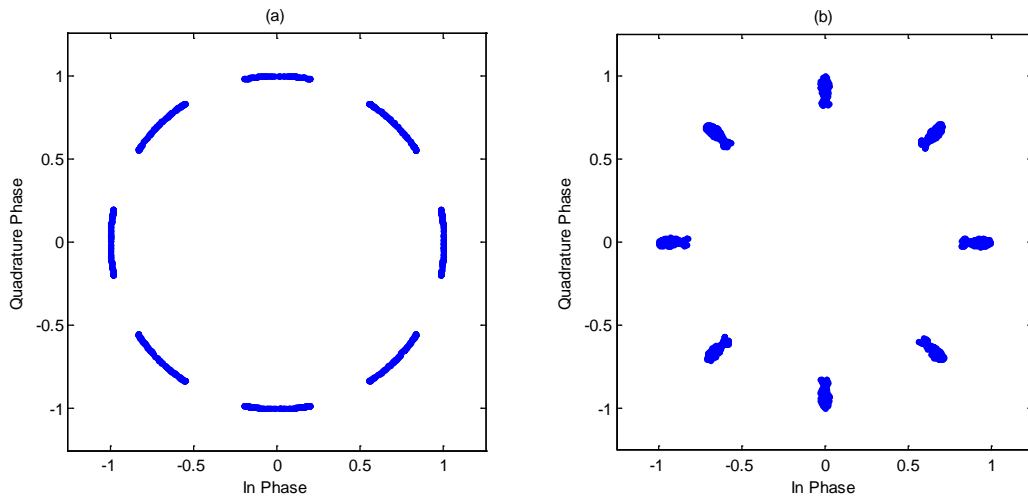


Fig. 6: Example constellation diagrams at the input (a) and output (b) of the system when a phase noise of 0.098 (with a constant probability density function) is added to the signal.

The regenerator was then fully characterized for various levels of initial Gaussian distributed phase noise added to the signal. The corresponding standard deviations of the phase and amplitude noise at the output of the system as a function of the input phase noise standard deviation are summarised in Fig.7. The output phase noise stays reasonably constant up to an input phase noise standard deviation of 0.065 radians, achieving a reduction in the phase noise by as much as 7.1 times. Beyond this value, the output phase noise slightly increases with input signal noise, however a reduction of almost 3 for the worst case we examined is still achieved, corresponding to an input phase noise standard deviation of 0.12 radians. The red dotted line denotes the 1:1 ratio and the region below it represents phase regeneration. On the other hand, if saturation is not achieved, phase-to-amplitude noise conversion takes place via the cosine transfer function shown in Fig. 3 (b). This effect can also be clearly

seen in Fig. 5 and Fig. 6. In our scheme, the PSA-based partial phase regenerator was intentionally operated in the linear regime to guarantee correct phase noise cancellation. Note, however, that this undesired phase-to-amplitude conversion effect could be reduced drastically if a more complex PSA scheme, including an extra phase harmonic, was considered, as proposed and demonstrated in [9, 10].

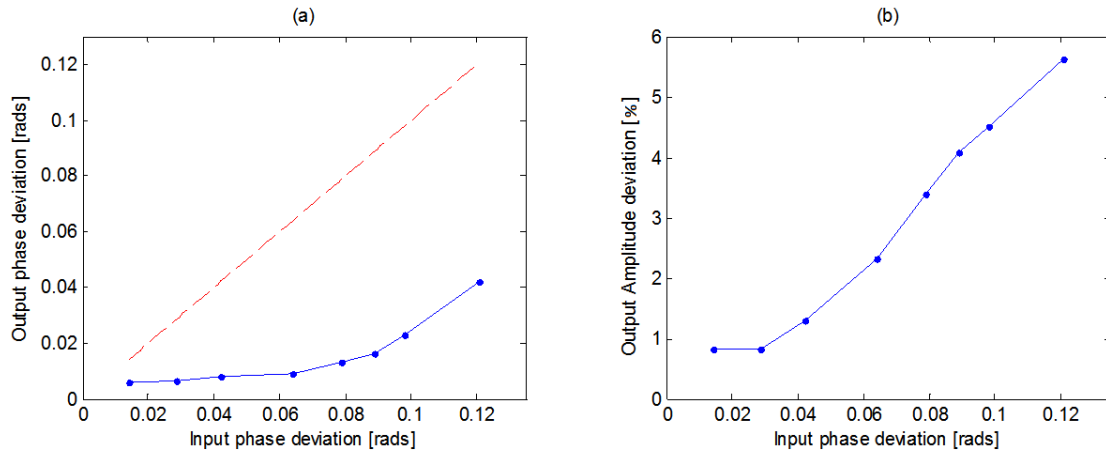


Fig. 7: Output phase standard deviations versus initial phase standard deviations (a) and normalized output amplitude standard deviations versus initial phase standard deviations (b).

Finally, the system was numerically characterized for the case when both Gaussian phase and amplitude noise was added to the 8-PSK input. The standard deviation of the phase and amplitude noise we assumed were 0.064 radians and 6%, respectively. Since the phase regenerator scheme amplifies the input amplitude noise, it was imperative to firstly reduce any amplitude noise present in the signal. To guarantee best overall performance an amplitude limiter based on a saturated single-pump parametric amplifier was added at the input of the proposed scheme. The amplitude limiter consisted of a single HNLFF (with the same characteristics as in the remaining sections), pumped by a CW signal with a power level of 27dBm at 1552 nm. The noisy 8PSK signal at its input had an average power of 23 dBm at 1557 nm. The amplitude limiter was successful in containing any strong amplitude noise distortion. Fig. 8 displays the corresponding constellation diagrams at the input (a) and output (b) of the 8-PSK regenerator. At the output of the regenerator the signal phase and amplitude noise deviations were 0.014 radians and 8.75%, respectively. Consequently, the phase deviation was reduced by a factor of 4.5, while the amplitude noise increased slightly by a factor of 1.5.

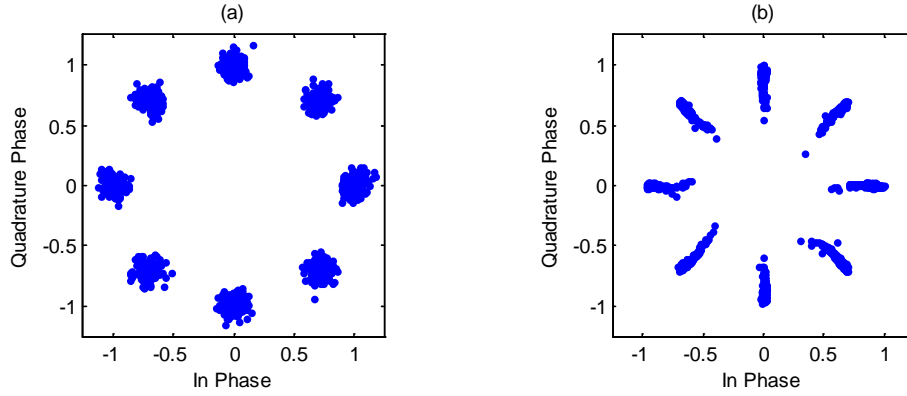


Fig. 8: Examples of constellation diagrams at the input (a) and output (b) of the system when Gaussian phase and amplitude noises with standard deviations of 0.064 radians and 6%, respectively, were added to the signal.

Some practical issues relating to this scheme are imposed by the need to preserve coherence among the different paths in the second stage of the system in Fig. 1. In our simulations, HNLFs have been considered, but we appreciate that in order to ensure that the signals traversing the various paths are added coherently, photonic integrated solutions would provide far better stability.

4. Conclusion

This work demonstrates a phase regeneration technique that allows an M-PSK signal to be regenerated using an M/2-PSK (or an even lower order) partial regenerator. The technique requires a three-stage coherent process. Firstly, a single pump parametric amplifier is used to produce the two spectral phase harmonics of interest, the second and third phase harmonics. Secondly, the second (down-converted) phase harmonic is partially regenerated using a M/2-PSK regenerator. Thirdly, the third phase harmonic and the partially regenerated second phase harmonic are used as the signal and pump, respectively, in a last FWM stage where the original signal is recovered at the very same wavelength.

5. Acknowledgments

This work is supported by the EPSRC grant EP/I01196X: Transforming the Future Internet: The Photonics Hyperhighway. FP gratefully acknowledges the support from the Royal Academy of Engineering/EPSRC through a University Research Fellowship.

6. References

- [1] R. Slavík, F. Parmigiani, J. Kakande, C. Lundström, M. Sjödin, P. A. Andrekson, R. Weerasuriya, S. Sygletos, A. D. Ellis, L. Grüner-Nielsen, and others, “All-optical phase and amplitude regenerator for next-generation telecommunications systems,” *Nat. Photonics*, vol. 4, no. 10, pp. 690–695, 2010.
- [2] F. Parmigiani, A. Bogris, D. Syvridis, J. Kakande, R. Slavík, R. Phelan, P. Petropoulos, and D. J. Richardson, “Multilevel quantization of optical phase in a novel coherent parametric mixer architecture,” *October*, vol. 5, no. October, 2011.
- [3] D. Mazroa, B. J. Puttnam, A. Szabo, S. Shinada, and N. Wada, “PPLN-based all-optical QPSK regenerator,” in *2013 15th International Conference on Transparent Optical Networks (ICTON)*, 2013, pp. 1–4.
- [4] T. Umeki, M. Asobe, and H. Takenouchi, “In-line phase sensitive amplifier based on PPLN waveguides,” *Opt. Express*, vol. 21, no. 10, pp. 12077–12084, 2013.
- [5] R. P. Webb, J. M. Dailey, R. J. Manning, and a D. Ellis, “Phase discrimination and simultaneous frequency conversion of the orthogonal components of an optical signal by four-wave mixing in an SOA,” *Opt. Express*, vol. 19, no. 21, pp. 20015–22, Oct. 2011.
- [6] A. Bogris and D. Syvridis, “All-optical signal processing for 16-QAM using four-level optical phase quantizers based on phase sensitive amplifiers,” *39th Eur. Conf. Exhib. Opt. Commun. (ECOC 2013)*, no. 1, pp. 501–503, 2013.
- [7] G. Lu, E. Tipsuwannakul, T. Miyazaki, C. Lundström, S. Member, M. Karlsson, and P. A. Andrekson, “Format Conversion of Optical Multilevel Signals Using FWM-Based Optical Phase Erasure,” *JLT*, vol. 29, no. 16, pp. 2460–2466, 2011.
- [8] J. Kakande, R. Slavík, F. Parmigiani, P. Petropoulos, and D. J. Richardson, “All-Optical Processing of Multi-level Phase Shift Keyed Signals,” *OFC*, vol. 4, no. 1, pp. 9–11, 2012.
- [9] G. Hesketh and P. Horak, “Reducing bit-error rate with optical phase regeneration in multilevel modulation formats,” *Opt. Lett.*, vol. 38, no. 24, pp. 5357–60, Dec. 2013.
- [10] K. R. H. Bottrill, G. Hesketh, F. Parmigiani, P. Horak, D. J. Richardson, and P. Petropoulos, “An Optical Phase Quantiser Exhibiting Suppressed Phase Dependent Gain Variation,” pp. 3–5.